CERN-PH-TH/2010-145, DCPT/09/152, DESY 10-154, IPPP/09/76,
KA-TP-35-2010

Higgs Production via Weak Boson Fusion in the Standard Model and the MSSM [1]

Terrance Figy[a2], Sophy Palmer[b3] and Georg Weiglein[c4]

[a]CERN, CH–1211 Geneva 23, Switzerland
[b]IThP, KIT, Universität Karlsruhe, 76128 Karlsruhe, Germany
[c]DESY, D–22603 Hamburg, Germany

Abstract

Weak boson fusion is expected to be an important Higgs production channel at the LHC. Complete one-loop results for weak boson fusion in the Standard Model have been obtained by calculating the full virtual electroweak corrections and photon radiation and implementing these results into the public Monte Carlo program `VBFNLO` (which includes the NLO QCD corrections). Furthermore the dominant supersymmetric one-loop corrections to neutral Higgs production, in the general case where the MSSM includes complex phases, have been calculated. These results have been combined with all one-loop corrections of Standard Model type and with the propagator-type corrections from the Higgs sector of the MSSM up to the two-loop level. Within the Standard Model the electroweak corrections are found to be as important as the QCD corrections after the application of appropriate cuts. The corrections yield a shift in the cross section of order 5% for a Higgs of mass 100–200 GeV, confirming the result obtained previously in the literature. For the production of a light Higgs boson in the MSSM the Standard Model result is recovered in the decoupling limit, while the loop contributions from superpartners to the production of neutral MSSM Higgs bosons can give rise to corrections in excess of 10% away from the decoupling region.

[1]Former address of the authors, where much of this work was carried out: IPPP, Durham University, Durham DH1 3LE, UK

[2]E-mail: Terrance.Maynard.Figy@cern.ch
[3]E-mail: Sophy.Palmer@particle.uni-karlsruhe.de
[4]E-mail: Georg.Weiglein@desy.de

1 Introduction

Weak boson fusion (WBF) is an important Higgs production channel at the LHC [1–3] and at a future Linear Collider [4, 5]. If the Higgs mechanism is responsible for generating the masses of the weak gauge bosons Z and $W^{\pm}$, one would expect that at least one Higgs boson should have a significant coupling to the weak bosons (unless the coupling to gauge bosons is shared among a large number of Higgs bosons, see e.g. [6]) and should therefore be produced in weak boson fusion. Besides its rôle as a discovery channel, it has also been shown that weak boson fusion production can provide important information on the couplings and $\mathcal{CP}$-properties of the detected state [7–9]. A precise theoretical prediction of this channel is mandatory in this context.

QCD corrections to weak boson fusion Higgs production at the LHC turned out to be moderate, at the level of 5% in the Standard Model (SM), and are theoretically well under control [3,10–17]. Additionally, uncertainties from parton distribution functions (PDFs) to this channel are quite small [3] in the phase space region relevant for the LHC. In view of the expected accuracies at the LHC [1,2,8] electroweak loop corrections may also be non-negligible. Besides the relevance of electroweak loop corrections for reducing the theoretical uncertainties of this channel, they are also of interest because of the potential effects of new physics entering via virtual contributions of additional particles in the loops. In the Minimal Supersymmetric Standard Model (MSSM), the most thoroughly studied extension of the SM, it has been shown for the case of Higgs production in weak boson fusion at a future linear collider that supersymmetric (SUSY) loop contributions can have a sizable impact on the production cross section [18]. In particular, the SUSY loop effects can significantly modify the decoupling behaviour of the VVH vertex, where $V = Z, W^{\pm}$, and H is the heavy $\mathcal{CP}$-even Higgs boson of the MSSM [18] (see also Ref. [18, 19] for leading SUSY loop corrections to the production of the light $\mathcal{CP}$-even Higgs boson in WBF at the Linear Collider; the complete one-loop contributions to the corresponding process in the SM have been obtained in Refs. [20–22]).

Electroweak loop corrections to Higgs production in WBF at the LHC have recently received considerable interest. In Refs. [23–25] the full one-loop electroweak and QCD loop corrections to the total cross section and differential distributions have been evaluated in the SM. The pure SUSY loop corrections to this process, without the SM part, have been obtained in [26, 27], and the SUSY-QCD corrections have also been investigated [28].

In the present paper we calculate the complete electroweak one-loop corrections to Higgs production in WBF at the LHC in the SM. We furthermore calculate corrections to the production of neutral Higgs bosons in the MSSM, combining the full one-loop SM-type contributions with the dominant SUSY one-loop corrections involving the scalar superpartners of the SM fermions and with the propagator-type corrections up to the two-loop level to the mass and wavefunction normalisation of the outgoing Higgs boson. For comparison with the dominant SUSY contributions from sfermions we have also calculated the full SUSY corrections to the VVh vertex, the weak boson self energies and the qqV vertices. We have implemented our results into the public Monte Carlo program `VBFNLO` [29] so that they can be used in experimental studies.

Our results go beyond the existing results in the literature in various ways. In particular, they incorporate loop effects from both SM and SUSY particles. Additionally, our SUSY loop corrections have been obtained for the general case of non-vanishing complex phases, which enables an analysis of the possible impact of $\mathcal{CP}$-violating effects. For comparison, we have furthermore evaluated the fermion and sfermion loop corrections to the production of the Z boson in WBF, which is of interest as a potential reference process to which WBF Higgs production could be calibrated. Where possible, we compare our results with those available in the literature.

2 Details of the calculation

2.1 Notations and conventions

The Higgs sector of the MSSM comprises two scalar doublets, resulting in five physical Higgs bosons. At lowest order the Higgs sector is $\mathcal{CP}$-conserving, giving rise to two $\mathcal{CP}$-even states h and H, a $\mathcal{CP}$-odd state A, and the charged Higgs bosons $H^\pm$. Besides the gauge couplings, the Higgs sector is characterised by two independent input parameters, conventionally chosen as M_A and $\tan\beta$ (in the case of $\mathcal{CP}$-violation one usually chooses $M_{H^\pm}$ instead of M_A as the input parameter). Here $\tan\beta$ is the ratio of vacuum expectation values of the two Higgs doublets. The other Higgs boson masses and the mixing angle α between the two neutral $\mathcal{CP}$-even states can be predicted in terms of the input parameters. Higher-order contributions yield large corrections to the masses and couplings, and can also induce $\mathcal{CP}$-violation

leading to mixing between h, H and A in the case of general complex SUSY-breaking parameters. The corresponding mass eigenstates are denoted as h_1, h_2, h_3.

The superpartners to the left- and right-handed fermions mix, yielding the mass eigenstates $\tilde{f}_1, \tilde{f}_2$. In the off-diagonal entries of the mass matrix the trilinear couplings A_f and the Higgsino mass parameter μ enter, which can be complex. Similarly, the mass eigenstates of neutralinos and charginos need to be determined from matrix diagonalisation, where the parameters M_1 and M_2 can be complex. The gluino mass and its phase enter our results only via the two-loop contributions to the Higgs propagators.

2.2 Types of corrections

In the following we describe details of the calculation of the one-loop electroweak corrections to WBF production of the SM Higgs boson $H^{\rm SM}$ and the MSSM Higgs bosons h, H, A (h_1, h_2, h_3) in the $\mathcal{CP}$-conserving ($\mathcal{CP}$-violating) case.[1] In the SM we take into account the complete one-loop electroweak corrections to the partonic $2 \to 3$ process, involving diagrams of pentagon, box, vertex and self-energy type. Generic types of virtual electroweak one-loop corrections, counterterm contributions and real photon emission are depicted in Fig. 1. These contributions have been implemented into the public Monte Carlo program `VBFNLO` [29], which contains the leading-order result supplemented by the one-loop QCD corrections in the SM. We therefore obtain results that contain the full one-loop QCD and electroweak corrections in the SM. In the MSSM we combine the SM-type contributions (i.e. from fermions, gauge bosons and the full MSSM Higgs sector) with the dominant loop corrections involving the scalar superpartners of the SM fermions. We evaluate these contributions for arbitrary complex phases. Going beyond the sfermion loop corrections, for the VVh_i vertex, the VV self energy and the qqV vertices, where $V = W^\pm, Z$ and $i = 1, 2, 3$, we have obtained the full one-loop contributions from all SUSY particles. For the propagator corrections to the mass and wavefunction normalisation of the outgoing Higgs boson, which are known to be sizable in the MSSM Higgs sector, we incorporate corrections up to the two-loop level as implemented in the program `FeynHiggs` [30–35]. The remaining SUSY loop corrections (the SUSY-QCD corrections and the SUSY pentagon and box diagrams involving the superpartners of the gauge

[1] Obviously, at leading order the $\mathcal{CP}$-odd Higgs A is not produced.

and Higgs bosons) will be presented in a forthcoming publication. They are expected to be of sub-leading numerical importance (see the discussion in [26]).

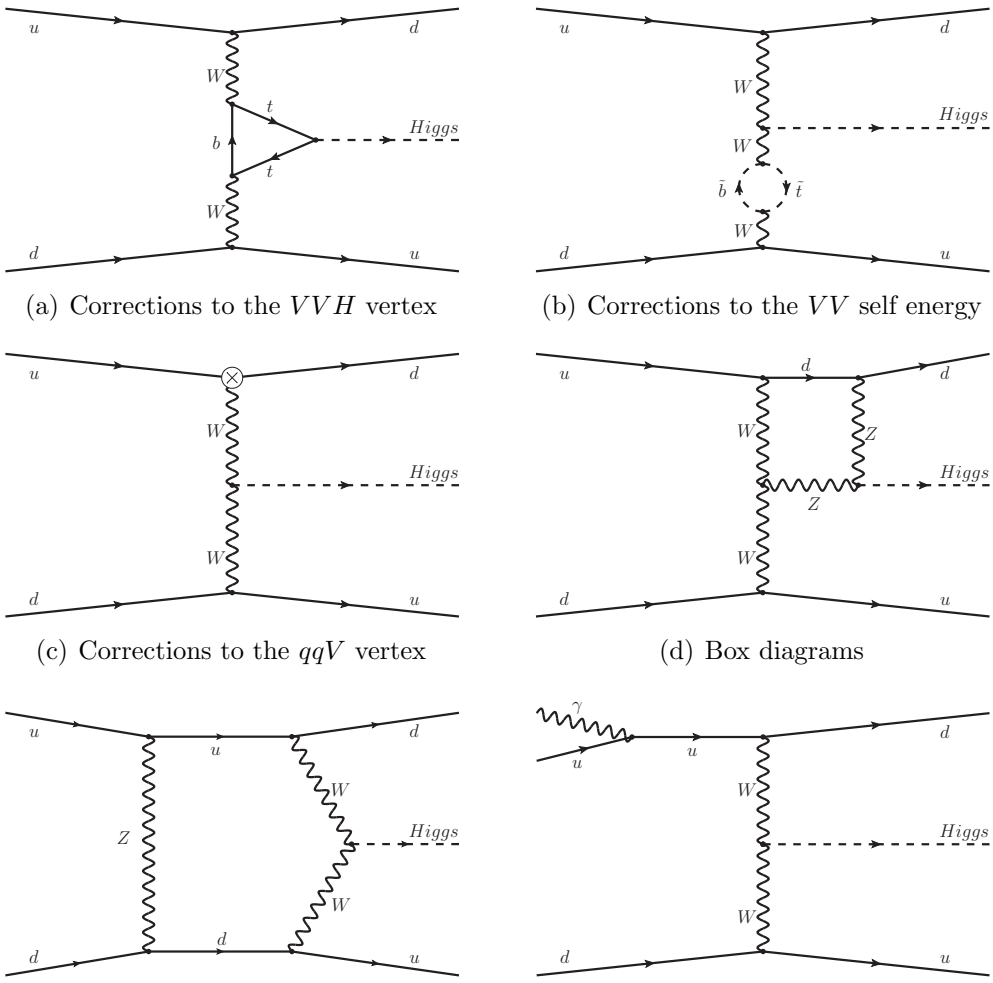

(a) Corrections to the VVH vertex

(b) Corrections to the VV self energy

(c) Corrections to the qqV vertex

(d) Box diagrams

(e) Pentagon diagrams

(f) Real photon emission

Figure 1: Types of electroweak corrections to the weak boson fusion process.

The virtual corrections are supplemented by the diagrams with real photon emission, see Fig. 1(f). The diagrams with real gluon emission (and the corresponding virtual corrections) are already included in `VBFNLO` [29].

In the SM, for the perturbative evaluation of the cross section up to the one-loop level, it is sufficient to take into account only the contributions of

the squared Born-level matrix element (as well as the one with real photon emission) and the product of the Born-level and the one-loop amplitude. In the MSSM, on the other hand, this is not necessarily the case. Since in particular for the production of the heavy Higgs bosons the Born-level matrix element can be very small (or even strictly zero in the case of the $\mathcal{CP}$-odd Higgs boson), the squared contribution of the loop amplitude, $|\mathcal{M}^{\text{loop}}|^2$, can be numerically relevant and needs to be incorporated.[2] The implementation of our results into `VBFNLO` is such that these corrections are automatically included in the MSSM calculation whenever the loop corrections are a sizeable fraction (greater than 15%) of the leading order contributions as, even when producing the lightest Higgs, they can be significant in the non-decoupling regime.

Besides the contributions to Higgs production in WBF we also consider higher-order corrections to the production of a Z boson in WBF at the partonic level. This process could in principle be of interest as a reference process (with a similar signature and, for a light Higgs, similar kinematics) to which Higgs production could be calibrated (see e.g. [36] for a discussion), although its experimental feasibility remains questionable at present [37]. We have calculated the fermion and sfermion loop corrections to this process (which is also incorporated, including one-loop QCD corrections, in `VBFNLO` [29]), which allows us to compare the pattern of the radiative corrections for the two processes.

The calculations of the Feynman diagrams were performed using the programs `FeynArts` [38, 39] and `FormCalc` [40–42], and the loop integrals were evaluated using `LoopTools` [43]. Throughout, we use Dimensional Reduction (DRED [44]).

2.2.1 Virtual corrections

The virtual corrections can be grouped into five different categories: corrections to the VVH vertex, corrections to the qqV vertex (where q is an external quark), weak boson self-energy corrections and box and pentagon diagrams, as shown in Fig. 1. Diagrams where the Higgs connects to one of the external quark lines are not considered as we work in the limit of vanishing external quark masses. Within the SM it has been found that the leading-order contribution where a Higgs is radiated off an external bottom

[2] The IR-divergent pieces are extracted prior to this procedure, see Sect. 2.2.3 below.

quark line can give rise to a correction of about 2% for a light Higgs [24]. In the MSSM the Higgs coupling to bottom quarks can be enhanced compared to the SM case. While the contributions on which we focus in this paper can easily be supplemented by the ones where a Higgs is radiated off an external bottom quark line, incorporation of the latter contributions would not change our qualitative discussion below.

We incorporate the corrections to the VVH vertex and the weak boson self energy by calculating an effective VVH coupling resulting from the loop and counterterm diagrams. The most general structure of the coupling between a pair of gauge bosons and a scalar particle is given by [12]

$$\begin{aligned} T^{\mu\nu}(q_1,q_2) &= a_1(q_1,q_2)g^{\mu\nu} + a_2(q_1,q_2)\left[(q_1q_2)\,g^{\mu\nu} - q_1^\mu q_2^\nu\right] + \\ &\quad a_3(q_1,q_2)\epsilon^{\mu\nu\rho\sigma}q_{1\rho}q_{2\sigma}. \end{aligned} \tag{1}$$

Here, q_1 and q_2 are the momenta of the weak bosons, and a_1, a_2 and a_3 are Lorentz invariant formfactors. At the tree level, only the formfactor a_1 has a non-zero value in the SM and the MSSM:

$$a^{\rm SM}_{1,H^{\rm SM}WW} = \frac{i\,eM_W}{\sin\theta_{\rm W}}, \tag{2}$$

$$a^{\rm MSSM}_{1,hWW} = \frac{i\,eM_W}{\sin\theta_{\rm W}}\sin(\beta-\alpha), \quad a^{\rm MSSM}_{1,HWW} = \frac{i\,eM_W}{\sin\theta_{\rm W}}\cos(\beta-\alpha). \tag{3}$$

At lowest order the MSSM formfactor a_1 for the lightest $\mathcal{CP}$-even Higgs boson differs from the SM value of a_1 by a factor $\sin(\beta-\alpha)$, which tends to 1 in the decoupling regime, i.e. for $M_A \gg M_Z$. The inclusion of higher order diagrams, however, gives rise to different contributions to a_1 in the two models, and in general yields non-zero values for a_2 and a_3. The approach of parametrising parts of the one-loop contributions in terms of formfactors has the advantage of being relatively simple, as well as being quick to calculate computationally. By running the formfactor calculation subroutines separately, the speed of parameter scans can be greatly enhanced, making it easier to identify interesting regions in the supersymmetric parameter space.[3]

We have calculated the corrections to the quark vertex in two different ways. If only the contributions from the (s)fermion sector are considered, an effective coupling can be used as there are only counterterm contributions in this case. When considering the complete corrections, on the other hand, we

[3]Interesting Higgs phenomenology is expected to manifest itself in these formfactors, owing to the differences between the SM and MSSM Higgs sectors.

calculate the full matrix element. Finally, the box and pentagon diagrams are included in `VBFNLO` by calculating the full $2 \to 3$ matrix elements.

In order to check these procedures for internal consistency, the corrections to the Higgs vertex have also been calculated using the full matrix elements instead of the simpler formfactor parametrisations, and we have verified that the two sets of results agree with each other.

2.2.2 Higgs propagator corrections

Higgs propagator corrections, which can be very important numerically, enter the prediction for the mass of the external Higgs boson and are furthermore required to ensure the correct on-shell properties of S-matrix elements involving external Higgs bosons, i.e. unit residue and vanishing mixing between different Higgs bosons on mass shell. It is convenient in this context to use finite wave function normalisation factors, which make it easy to incorporate leading higher-order contributions. A vertex function with an external Higgs boson h_a ($a = 1, 2, 3$) in general receives contributions from all three lowest-order neutral Higgs states[4] according to

$$\begin{pmatrix} \hat{\Gamma}_{h_1} \\ \hat{\Gamma}_{h_2} \\ \hat{\Gamma}_{h_3} \end{pmatrix} = \hat{\mathbf{Z}} \cdot \begin{pmatrix} \hat{\Gamma}_{h} \\ \hat{\Gamma}_{H} \\ \hat{\Gamma}_{A} \end{pmatrix}, \tag{4}$$

where the elements of the (non-unitary) matrix $\hat{\mathbf{Z}}$ have been defined in [33, 45]. In the $\mathcal{CP}$-conserving case mixing occurs only between the two $\mathcal{CP}$-even states. We calculate the wavefunction normalisation factors and the Higgs boson masses using the program `FeynHiggs`, taking into account the full one-loop result as well as the dominant two-loop contributions.

In our numerical discussion below we incorporate the universal wavefunction corrections into the lowest order matrix element, so that the effect of the genuine one-loop corrections can be discussed separately from the known propagator-type contributions. Accordingly, in the following we use the phrase "leading order" for the tree-level element supplemented by the wavefunction normalisation factors (and parametrised in terms of the loop-corrected mass of the outgoing Higgs boson), whereas "tree" refers to the

[4] In general, one also needs to consider mixing with Goldstone bosons. For the case of weak boson fusion, however, no such contributions occur at the one-loop level and we therefore do not consider them here. For completeness, contributions due to mixing with gauge bosons are included in the calculation, although they are not significant numerically.

purely tree level diagrams without the wavefunction normalisation factors (parametrised also in this case in terms of the loop-corrected Higgs mass).

In principle there is a choice between treating the universal wavefunction corrections as an "additive" correction, i.e. absorbing them into the tree-level part of the amplitude only, or as a "multiplicative" correction, i.e. applying them both to the tree-level and the one-loop part of the amplitude. The difference between the two options is of higher order. For the results shown below, in which the wavefunction corrections are treated as "additive", the numerical difference between the two options is insignificant. Sizable effects are possible, however, in "extreme" regions of the parameter space, for instance in the non-decoupling regime of $\mathcal{CP}$-violating scenarios. In cases like this the inclusion of the wavefunction corrections in the loop part of the amplitude can have an impact on the shape of azimuthal angle distributions. As the universal wavefunction corrections are not the main focus of the present paper, we will not discuss this issue any further here.

2.2.3 Real corrections

As mentioned above, we work in the limit of vanishing quark mass for the external (1st and 2nd generation) quarks. We regularise the IR and collinear divergences by a small photon mass and small quark masses, respectively, and use the dipole subtraction formalism as described in [46]. As an additional check on the IR finiteness of the results, we have also implemented the soft photon approximation (see e.g. [47]) as an alternative to dipole subtraction. Matrix elements for processes with real photon emission have been calculated using helicity amplitudes [48], and have been numerically compared with matrix elements generated with `Madgraph` [49] for individual phase space points.

2.3 Renormalisation

We perform the renormalisation of the parameters and fields as outlined in [33]. While the algebraic structure of the counterterms for the qqV vertex and VV self energy are the same in the MSSM as in the SM, the counterterms for the VVH vertices contain contributions from the renormalisation of $\tan\beta$ and off-diagonal contributions from the Higgs field renormalisations. For the $\mathcal{CP}$-conserving case the explicit form of these counterterms has been given in [18]. In the $\mathcal{CP}$-violating case there are non-zero counterterm con-

tributions for all three vertices of the kind VVh_a, $a = 1, 2, 3$. The relevant MSSM counterterms were implemented into a `FeynArts` model file. The implementation of our results into `VBFNLO` has three options for parametrising the electromagnetic coupling in the Born level cross section. In the code the electromagnetic coupling can be parameterised by $\alpha(0)$, $\alpha(M_Z)$ and via the Fermi constant, G_F. In the latter case the relation

$$\alpha \equiv \alpha(0) = \frac{\sqrt{2} G_F M_W^2}{\pi \left(1 + \Delta r\right)} \left(1 - \frac{M_W^2}{M_Z^2}\right) \tag{5}$$

is employed, where the quantity Δr contains higher-order corrections to muon decay, see [50, 51]. The charge renormalisation counterterm is adjusted according to the chosen option.

We have checked that the UV divergences cancel not only for the full result but also separately for the (s)top / (s)bottom and for the (s)fermion contributions. Furthermore we have verified for the (s)fermion contributions that the corrections from the qqV vertex, the weak boson self energy and the VVH vertex are all separately finite. We have also checked, algebraically and numerically, that the weak boson field renormalisation constants drop out in the sum of all counterterm contributions. The parameters used for regularising the UV divergence and the IR divergencies (quark mass and photon mass) can all be varied numerically in the code. We have verified that our result has no dependence on any of these parameters.

3 Numerical results

Unless otherwise stated, we use the PDF set MRST2004qed [52], as this includes QED corrections (thus allowing photon induced processes to be considered), the gauge coupling is parametrised by G_F, and a centre of mass energy of 14 TeV is used. We normally set $m_t = 172.6$ GeV [53], and for the other parameters we use the values given by the Particle Data Group [54]. By default, we use M_W as both the renormalisation and factorisation scale.

3.1 Cuts and non-WBF processes

By default, the cuts used here are those described in [24]:

$$\begin{aligned} p_{T_j} &> 20 \text{ GeV} \\ |\, y_j \,| &\geq 4.5 \\ \Delta y_{ij} \equiv| \, y_{j_1} - y_{j_2} \,| &> 4 \\ y_{j_1} \cdot y_{j_2} &< 0, \end{aligned} \tag{6}$$

where p_{T_j} is the transverse momentum of a jet, and y_j is its rapidity. In addition, the k_T algorithm is used to reconstruct jets from the final state partons, using the parameters

$$\begin{aligned} R_{jj} &\geq 0.8 \\ |\, \eta \,| &< 5, \end{aligned} \tag{7}$$

where R_{jj} is the R separation of the two jets, and η is the pseudorapidity of the partons. These cuts ensure that the signal is relatively clean and that the effect of processes such as the s-channel Higgsstrahlung process is small [15, 24, 55]. Consequently, the Higgsstrahlung process is not included in this work.

3.2 Comparison with the literature

As a first step, the leading order result in the SM was checked against the result obtained using `MadGraph` [49]. The results were found to agree to within the numerical accuracy of the respective codes. Additionally, the tree-level matrix elements for Higgs production via weak boson fusion plus a photon were also compared with [56], and found to be in full agreement.

We next compare the complete one-loop result for the weak boson fusion channel in the SM with the result obtained in Ref. [24]. Accordingly, we compare our result with the t-channel contribution given by the code `HAWK`, which was developed in Ref. [24].[5] Table 1 shows a comparison for on-shell Higgs production between `VBFNLO`, incorporating our results, and the result

[5]Contributions from the s-channel and t/u interference are numerically small, below the level of ∼0.5%, once weak boson fusion cuts have been applied. We furthermore have not included photon induced processes in this comparison, as in general their s- and t-channel contributions are not separately gauge-invariant, but we have verified that our results for the photon induced processes are in good agreement with Ref. [24].

Table 1: Comparison of our results, as implemented into the code `VBFNLO` (labelled "this work"), for the leading order (LO) cross section and the full one-loop contribution (NLO, containing both QCD and electroweak corrections) to the weak boson fusion (t) channel with those obtained using `HAWK`, the code developed in Ref. [24].

M_H [GeV]	120	150	200
σ_{LO}, `HAWK` [fb]	1876.96 ± 1.59	1589.87 ± 1.25	1221.40 ± 0.87
σ_{LO}, this work [fb]	1876.66 ± 1.32	1590.19 ± 1.10	1221.26 ± 0.82
σ_{NLO}, `HAWK` [fb]	1637.85 ± 3.22	1387.36 ± 2.40	1074.14 ± 1.72
σ_{NLO}, this work [fb]	1634.54 ± 2.39	1387.37 ± 2.09	1073.08 ± 1.54

obtained using `HAWK`, with all parameters and cuts set to match Ref. [24]. Table 1 shows that both the leading order results of the two codes as well as the predictions for the cross section including the complete QCD and electroweak one-loop corrections in the SM fully agree with each other within the numerical uncertainties.

We now turn to the comparison with the results for the purely supersymmetric corrections to weak boson fusion in the MSSM with real parameters given in Ref. [26]. The separation into "pure SUSY" and "SM-type" contributions can easily be performed as long as one only considers loop contributions from SM fermions and their scalar superpartners. Going beyond the (s)fermion contributions, however, this distinction is less obvious owing to the increased complexity of the Higgs sector in the MSSM as compared to the SM case. The authors of Ref. [26] have chosen to define the "pure SUSY" corrections for the production of the light $\mathcal{CP}$-even Higgs boson according to

$$\sigma_{SUSY} = \sigma_{MSSM} - \sin^2(\beta - \alpha)\, \sigma_{SM}, \tag{8}$$

which ensures that σ_{SUSY} contains only IR-finite virtual contributions (the factor $\sin^2(\beta - \alpha)$ is the ratio of the squared lowest order coupling of the light $\mathcal{CP}$-even Higgs to two weak bosons over the corresponding coupling of a SM Higgs, see Eqs. (2), (3)). In comparing with Ref. [26] we focus on the supersymmetric contributions to the VVh vertex.[6] Table 2 shows a

[6]Here, as in Ref. [26], we include contributions from photon fusion and photon-Z fusion.

Table 2: Comparison of percentage corrections to the total Higgs production cross section arising from contributions to the VVh vertex of pure SUSY type, defined according to Eq. (8), with the results presented in Ref. [26]. The column labelled "This work" gives our results, incorporating Higgs propagator corrections up to the two-loop level. The column labelled "Tuned result" was obtained by adapting our calculation to the prescriptions used in Ref. [26] (see text). The column labelled "Propagator-type corrections" gives the percentage correction arising from the universal wavefunction normalisation factors, see Sect. 2.2.2. The right-most column shows the results as given in Ref. [26].

SPS	This work	Tuned result	Propagator-type corrections	Ref. [26]
1a	-0.210	-0.365	3.231	-0.329
1b	0.044	-0.204	3.431	-0.162
2	-0.046	-0.224	3.539	-0.147
3	-0.028	-0.214	3.557	-0.146
4	-0.065	-0.274	3.173	-0.258
5	-0.651	-0.619	1.970	-0.606
6	-0.108	-0.281	3.395	-0.226
7	-0.052	-0.246	3.691	-0.206
8	-0.007	-0.216	3.766	-0.157
9	0.031	-0.190	3.956	-0.094

comparison of our results with the ones of Ref. [26] for the relative impact of the pure SUSY loop corrections, defined according to Eq. (8), on the total Higgs production cross section. In order to enable a comparison with the relative corrections given in Ref. [26] we have expressed the Higgs propagator corrections (see Sect. 2.2.2) as part of the loop contributions rather than absorbing them into the leading order result as we do elsewhere in this paper.[7]

There are several differences between our approach and that used in Ref. [26], related in particular to the treatment of higher-order corrections in the Higgs sector. We use the tree level Higgs masses and mixing angle for all Higgs bosons occuring within loop diagrams,[8] whereas Ref. [26] uses

[7]It turns out that our result for the leading order cross section differs from the value stated in Ref. [26].

[8]This ensures the UV finiteness of the Higgs self energies.

loop-corrected masses and couplings. In our work, we incorporate contributions up to the two-loop order in the Higgs propagator-type corrections entering the predictions for the Higgs masses and the Higgs wavefunction normalisation factors (see Sect. 2.2.2), while in Ref. [26] the contributions to the Higgs field renormalisations are restricted to the one-loop level. A further difference arises from the fact that we focus on the vector boson fusion process, whereas Ref. [26] also includes Higgsstrahlung contributions (as discussed above, since weak boson fusion cuts are applied the impact of the latter contributions is numerically small). We have added a column labelled "Tuned result" in Table 2 that has been obtained using a specially tuned version of our code, where the treatment of the higher-order corrections in the Higgs sector has been performed in accordance with the prescription in Ref. [26].[9]

The comparison in Table 2 has been carried out for the SPS benchmark points [57], where the same low-energy input parameters have been used as in Ref. [26]. Furthermore, the electromagnetic coupling constant is set to $\alpha(0)$, the PDF set MRST2002nlo [58] is applied, the top mass is set to $m_t = 170.9$ GeV, the renormalisation and factorisation scale is set to M_h, and the same set of cuts is used as in Ref. [26]. For illustration, in the column labelled "Propagator-type corrections" in Table 2 we separately show the percentage loop correction arising from the universal wave function normalisation factors (see Sect. 2.2.2).

The relative corrections for the different SPS benchmark points shown in Table 2 are found to be rather small, well below the level of 1%. This turns out to be a consequence of large cancellations between the universal propagator-type corrections, which are at the level of 3–4%, as seen in the fourth column of Table 2, and the process-specific genuine vertex corrections.[10] The latter tend to overcompensate the positive correction arising from the propagator-type contributions, yielding overall a negative correction at the sub-percent level for most of the SPS points. It should furthermore be noted in this context that all SPS points belong to the decoupling region of the supersymmetric parameter space, where the couplings of the light $\mathcal{CP}$-even Higgs are SM-like, i.e. no large SUSY loop effects on the Higgs couplings are expected in this parameter region. The comparison between our results

[9] Note that slightly different versions of `FeynHiggs` were used, leading to small differences in the values of the Higgs parameters.

[10] Note that the propagator corrections used in this comparison are larger than those used in the rest of this paper, owing to a different scale choice.

(labelled as "This work") and the ones quoted in Ref. [26] shows reasonably good agreement, with absolute deviations at the level of 0.2% or below. The agreement further improves if our "Tuned result" (where the treatment of the higher-order corrections in the Higgs sector has been performed in accordance to the prescription in Ref. [26], as explained above) is used for the comparison. The remaining deviations between the "Tuned result" and the results of [26] are likely due to a combination of small factors, such as slight remaining differences in the calculation of the Higgs sector, the inclusion of additional diagrams, and the numerical inaccuracy inherent in the Monte Carlo integration.

3.3 Total cross sections and distributions

Figure 2(a) shows the total cross section in the Standard Model for a range of M_H, obtained from `VBFNLO` incorporating our results. The curve labelled "tree + full corrections" shows the full one-loop result in the SM for Higgs production in weak boson fusion at the LHC with 14 TeV, using the input values and cuts as specified above. The full one-loop result is compared with the tree-level result (labelled "tree"), the result incoporating only QCD corrections ("tree + QCD corrections") and the result incorporating in addition fermion-loop corrections ("tree + QCD + fermion corrections"). For illustration the full result is also shown for energies of 10 TeV and 7 TeV, corresponding to a reduction of the cross section by a factor of approximately 1.8 and 3.8 respectively (for a Higgs mass of 120 GeV compared to the cross section at 14 TeV). Figure 2(b) shows the percentage corrections. One can see from the plot that the QCD and the electroweak corrections are of similar size, being of order 5%, and enter with the same sign. It is interesting to note that the non-fermion contributions to the loop corrections are significant, causing a further reduction in the cross section. In our parametrisation of the result, the (bosonic) box- and pentagon-type contributions turn out to be numerically small. In Figure 2(b), the thresholds at $M_H = 2M_W$ and $M_H = 2M_Z$ are clearly visible. The reduction in the percentage corrections for lower centre of mass energies originates primarily in the QCD corrections.

As an example for a differential distribution we show the azimuthal angle distribution in Figure 3. This distribution is of particular interest in determining the structure of the coupling between the Higgs boson and the weak boson pairs [59], since its shape is in principle sensitive to the relative values of the formfactors a_1, a_2 and a_3, as defined in Eq. (1). The distribution is

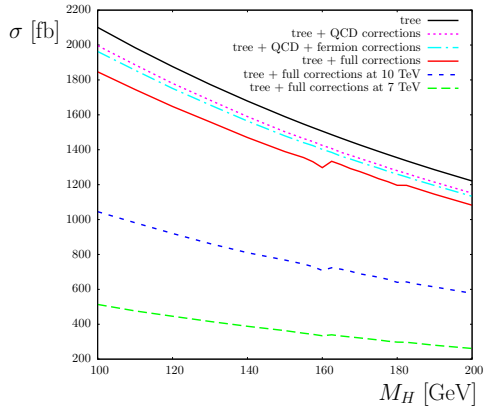

(a) Total cross section for Higgs production as a function of M_H in the Standard Model.

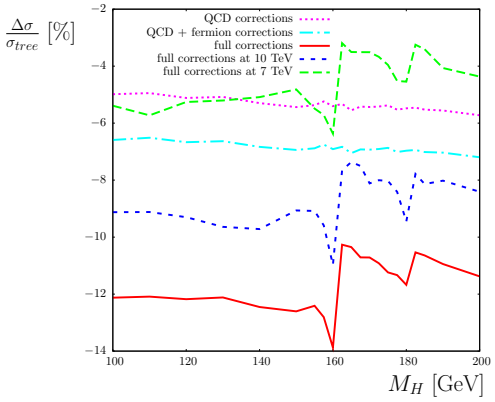

(b) Percentage higher order corrections for Higgs production as a function of M_H in the Standard Model.

Figure 2: Results for Higgs boson production via weak boson fusion in the Standard Model. The full one-loop result, labelled "tree + full corrections" is compared with various approximations (see text).

shown for a mass $M_H = 120$ GeV in the SM. The relative impact of the different types of corrections is as in Figure 2(a) (here, we also present the result containing the contributions from the third generation quarks in addition to the QCD corrections ("tree + QCD + t/b corrections"), which shows that the fermion loop contributions are dominated by the third generation quarks). The shape of the distribution turns out to be affected only mildly by the higher-order corrections. This can be understood from the fact that only the formfactor a_1 receives significant corrections in the SM, at the level of 1–2%, while the formfactors a_2 and a_3 in the SM are extremely small (approximately 5 and 10 orders of magnitude smaller than Δa_1 respectively) so that the corresponding effects will not be experimentally detectable at the LHC [60].

Moving to the case of the MSSM, we first investigate the impact of the loop corrections from fermions and sfermions on the formfactors a_1, a_2, a_3 for the WWh vertex. This is shown in Fig. 4, where the MSSM predictions in different benchmark scenarios are given as a function of $\tan\beta$ for $M_A = 150$ GeV. The ($\mathcal{CP}$-conserving) $M_h^{\rm max}$, no-mixing, small $\alpha_{\rm eff}$ and gluophobic benchmark scenarios have been defined in Ref. [61], while for the ($\mathcal{CP}$-violating) CPX scenario we use the definition given in Ref. [62], except that for the trilinear coupling parameter A_t we use the (on-shell) value

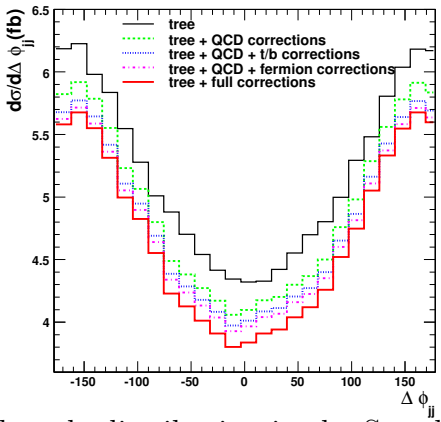

Figure 3: Azimuthal angle distribution in the Standard Model, with $M_H = 120$ GeV. The full one-loop result, labelled "tree + full corrections" is compared with various approximations (see text).

of 900 GeV (for the CPX scenario we use $M_{H^\pm} = 150$ GeV rather than $M_A = 150$ GeV). For comparison, the result in the SM is also shown, where the value of the Higgs mass has been set to the value obtained for the light $\mathcal{CP}$-even Higgs mass in the $M_h^{\rm max}$ scenario.

Fig. 4(a) illustrates that the corrections to a_1 can be larger in the $\mathcal{CP}$-conserving benchmarks than in the SM case, but are still typically of the order of a few per cent (note that, unlike in Sect. 3.2, these results include all fermion and sfermion diagrams involved in the corrections to the formfactors, rather than the purely supersymmetric corrections). The situation is different in the CPX scenario, see Fig. 4(b), where a_1 has an exceedingly small value in certain regions of parameter space, due to the loop-induced mixing between the three neutral Higgs bosons. As in the SM case, the contributions to a_2 and a_3 (see Fig. 4(c), 4(d)) turn out to be very small.[11]

We next consider the total cross section for the production of the light MSSM Higgs boson h in the $M_h^{\rm max}$ scenario as a function of M_A. We begin in Fig. 5 by comparing the leading order (LO) cross section in the MSSM (as explained above, the LO cross section contains the effect of the universal wavefunction normalisation factors and is evaluated at the loop-corrected

[11] Note that, as expected, the sfermions do not contribute to the value of a_3. The behaviour of a_3 as a function of $\tan\beta$ is purely the result of different couplings to the Higgs boson.

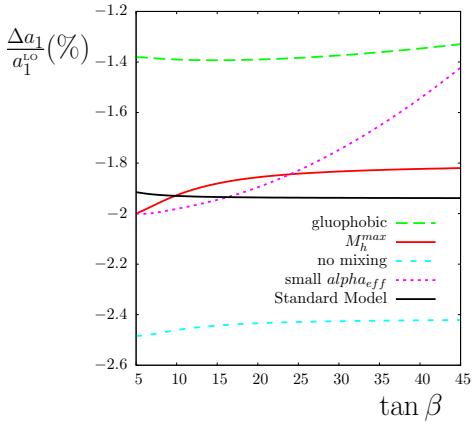

(a) Loop corrections Δa_1 to the formfactor a_1 as a percentage of the tree level, $a_1^{\rm LO}$, for benchmarks in the MSSM with real parameters.

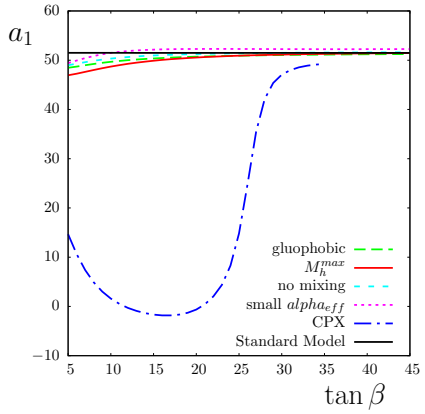

(b) Corrected value of the formfactor a_1 for all benchmarks.

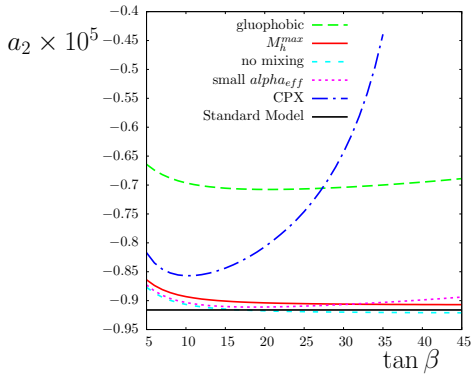

(c) Value of the formfactor a_2.

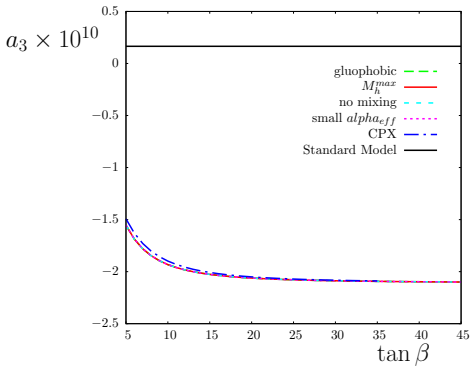

(d) Value of the formfactor a_3.

Figure 4: Corrections from fermion and sfermion loops to the formfactors of the WWh_1 vertex in the MSSM as a function of $\tan\beta$, with $M_A = 150$ GeV (for the CPX scenario, $M_{H^\pm} = 150$ GeV is used). For comparison, the SM formfactors are also shown, with a Higgs mass that matches the light $\mathcal{CP}$-even Higgs mass in the $M_h^{\rm max}$ scenario.

value of the Higgs mass) with the prediction where SM QCD corrections are included (labelled "LO + QCD corrections") and with the predictions where in addition the loop corrections from the third generation quarks and their scalar superpartners ("LO + QCD + (s)t/b corrections") and from all three generations of quarks and leptons and their scalar superpartners ("LO +

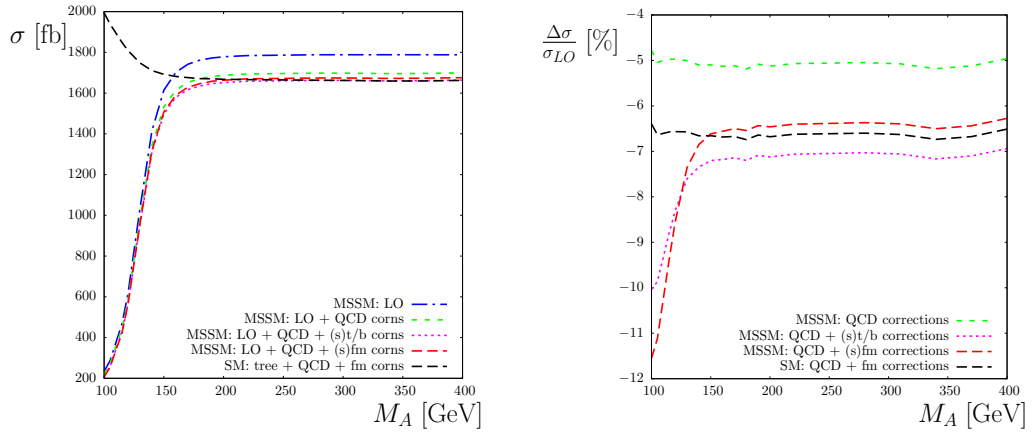

(a) Total cross section. (b) Percentage corrections.

Figure 5: Light Higgs boson h production as a function of M_A in the $M_h^{\max}$ scenario, with $\tan\beta = 10$.

QCD + (s)fermion corrections") are included. The range in M_A displayed in Fig. 5 represents a variation in the mass of the lightest Higgs boson from ≈ 98 GeV to ≈ 130 GeV. For comparison, the Standard Model cross section for the corresponding value of the Higgs mass is also shown. Fig. 5(b) shows the relative size of the higher-order corrections, normalised to the leading-order prediction (we parametrise the leading order cross section in terms of the Fermi constant G_F, see Eq. (5), taking into account the appropriate contributions to Δr in the SM and the MSSM).

It is well known that in the decoupling limit, i.e. for $M_A \gg M_Z$, the light $\mathcal{CP}$-even MSSM Higgs boson behaves in an SM-like fashion. This feature can clearly be seen in Fig. 5, where for $M_A \gtrsim 150$ GeV the MSSM cross section including QCD corrections and fermion / sfermion loop contributions is very close to the corresponding SM cross section (incorporating QCD corrections and fermion loop contributions). As in the SM case, the incorporated corrections are at the level of -6% in this region. For small M_A, on the other hand, the couplings of the light $\mathcal{CP}$-even Higgs deviate significantly from the SM case, giving rise to a suppression of the WBF production of h (while production of the heavy $\mathcal{CP}$-even Higgs boson, H, becomes relevant in this region, see below). The relative size of the loop corrections is much larger in this region compared to the decoupling region, exceeding -11% for small M_A.

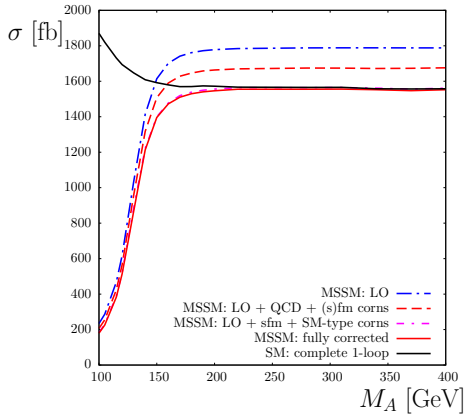

(a) Total cross section in the MSSM, incorporating different kinds of corrections, compared with the complete one-loop result in the SM.

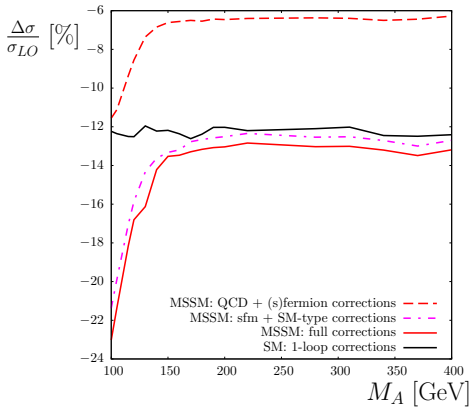

(b) Percentage loop correction.

Figure 6: Light Higgs boson h production as a function of M_A in the $M_h^{\max}$ scenario, with $\tan\beta = 10$. The most complete MSSM result ("MSSM: fully corrected") incorporates all one-loop SM-type corrections as well as all sfermion loop contributions and the further MSSM corrections to the VVh, VV and qqV contributions. The leading order (LO) result and results containing different parts of the higher-order corrections are also shown. The numerical uncertainties of the Monte Carlo integration on the corrected cross section are at the per-mille level.

Moving beyond the electroweak corrections from fermion and sfermion loops, we now present our most complete prediction for WBF Higgs production in the MSSM. We incorporate all SM-type corrections, i.e. the NLO QCD corrections already present in `VBFNLO` together with the self-energy, vertex, box and pentagon contributions involving the gauge bosons, leptons, quarks and the particles of the MSSM Higgs sector, as well as the real photon radiation.[12] Since we treat the external quarks of the WBF process to be massless, no Higgs or Goldstone bosons appear in the loops of the box and pentagon contributions, so that those contributions are the same as in the SM case, except for the modified coupling of the outgoing Higgs boson. Those SM-type corrections are combined with the sfermion loop contributions in the MSSM. The corresponding result is shown for WBF production of the

[12] As discussed above, the SM-type contributions beyond the fermion loops play a significant role in this context.

light $\mathcal{CP}$-even Higgs boson in Fig. 6, labelled as "MSSM: LO + sfermion + SM-type corrections". For illustration, we also show the prediction where furthermore the full MSSM corrections to the VVh, VV and qqV contributions are taken into account, labelled "MSSM: fully corrected". Accordingly, the "MSSM: fully corrected" result differs from the complete one-loop result in the MSSM only in that we neglect the SUSY QCD (i.e. gluino-exchange) contributions as well as contributions from charginos and neutralinos to the box and pentagon corrections.[13] The MSSM results are compared with the complete one-loop result in the SM for the corresponding value of the Higgs mass. Furthermore, the leading order result in the MSSM and the result incorporating QCD and fermion / sfermion loop corrections, both already shown in Fig. 5, are also displayed.

One can see in Fig. 6 that the result including the full SM-type corrections as well as the sfermion loop contributions ("MSSM: LO + sfermion + SM-type corrections") is very close to the one where the remaining MSSM one-loop corrections to the VVh, VV and qqV contributions are also taken into account ("MSSM: fully corrected"). In fact, the contribution from charginos and neutralinos amounts to a correction of only $\sim 0.3\%$ in the decoupling regime, and is slightly larger in the non-decoupling regime. It seems reasonable to expect that, as for the VVh, VV and qqV corrections, the contribution from charginos and neutralinos will have a relatively small effect on the boxes and pentagons. The calculation and implementation of the full result in the MSSM (including also the SUSY QCD contributions) will be presented in a forthcoming publication, but the result presented here should serve as a good approximation to the complete one-loop result in the MSSM (supplemented by higher-order propagator-type contributions), except possibly in parameter regions with a rather light gluino.

In the right plot of Fig. 6 the relative effect of the various contributions is shown. The SM-type contributions beyond the QCD and fermion / sfermion loop corrections can be seen to give rise to a downward shift of the cross section by about -6% in the decoupling region ($M_A \gg M_Z$). As before, the MSSM result for the light $\mathcal{CP}$-even Higgs boson in the decoupling limit is found to converge to the SM result with the corresponding value of the Higgs mass. The deviation between the relative corrections in the SM and in

[13] As above, the leading order cross section is parameterised in terms of the Fermi constant G_F. For the evaluation of the quantity Δr in the MSSM we neglect contributions from charginos and neutralinos.

the MSSM, indicating the impact of the additional SUSY loop contributions present in the MSSM, is at the level of 0.8% in this region. In the non-decoupling regime, on the other hand, the loop effects in the MSSM can differ from those in the SM by more than 10% (it should be noted, of course, that the relative size of the loop contributions is largest in the parameter region where the production cross section for the light $\mathcal{CP}$-even MSSM Higgs boson is most heavily suppressed as compared to the SM case).

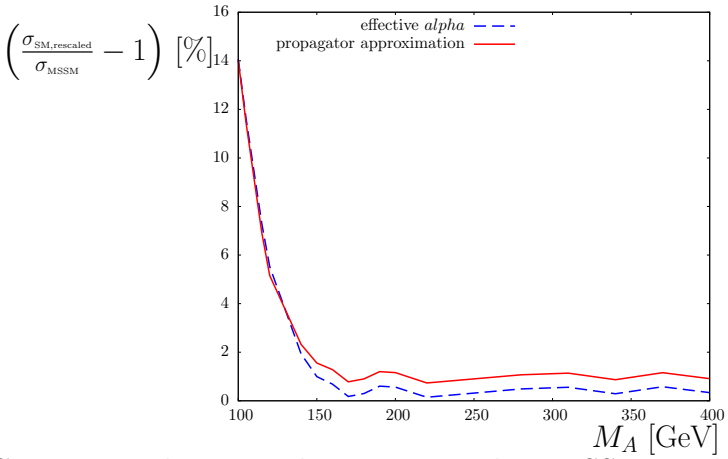

Figure 7: Comparison between the most complete MSSM result for h production with predictions where the complete one-loop result in the SM has been rescaled by the propagator-type corrections in the MSSM (solid red line) and by the effective coupling factor $\sin^2(\beta - \alpha_{\rm eff})$ (dashed blue line). The parameters are the same as in Fig. 6.

An approximate treatment widely used in the literature for obtaining MSSM predictions for Higgs production cross sections is to supplement the loop-corrected cross section for Higgs production in the SM with an appropriate scaling factor. For weak boson fusion, a possible scaling factor is obtained from the Higgs propagator-type contributions (written here for the $\mathcal{CP}$-conserving case; a generalisation to the case where all three neutral MSSM Higgs bosons mix with each other is easily possible)

$$\sigma_{\rm MSSM} \sim |\sin(\beta - \alpha_{\rm tree}) Z_{hh} + \cos(\beta - \alpha_{\rm tree}) Z_{hH}|^2 \; \sigma_{\rm SM}. \tag{9}$$

Approximating the wave function normalisation factors further (see for instance Ref. [63]) leads to a simple effective coupling factor which rescales the SM cross section,

$$\sigma_{\rm MSSM} \sim \sin^2(\beta - \alpha_{\rm eff}) \; \sigma_{\rm SM}. \tag{10}$$

In Fig. 7 we consider the approximation where the complete one-loop result in the SM is rescaled as described above (labelled "propagator approximation" and "effective alpha", respectively) and compare the resulting prediction with our most complete MSSM result as given in Fig. 6. As expected, in the decoupling region, $M_A \gg M_Z$, where h becomes SM-like, the simple rescaling of the loop-corrected SM result provides a good approximation of the MSSM prediction (it turns out that in this particular scenario the SM result scaled with $\sin^2(\beta - \alpha_{\text{eff}})$, which involves additional approximations, happens to be closer to the most complete MSSM result than for the case where the scaling factor based on the Higgs propagator contributions is used). On the other hand, for lower M_A we find significant deviations of up to $\sim 15\%$.

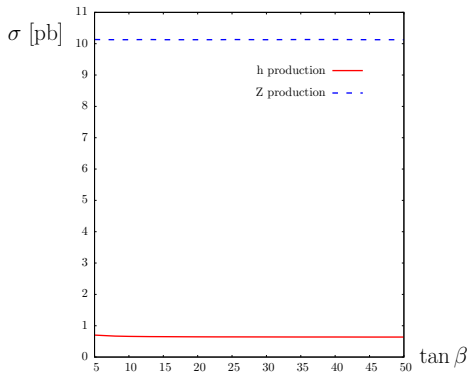

(a) Partonic h and Z production cross sections including (s)fermionic corrections as a function of $\tan\beta$.

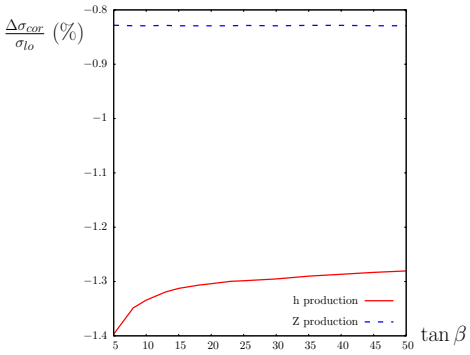

(b) Effect of the fermionic and sfermionic loop corrections relative to the leading order cross sections for h and Z production.

Figure 8: Partonic cross sections for h and Z production in the M_h^{max} scenario incorporating (s)fermionic corrections, with $M_A = 150$ GeV at $\sqrt{\hat{s}} = 500$ GeV.

As discussed above, we have also calculated the fermion and sfermion loop corrections to the process where a Z boson is produced in WBF, which in principle could be used as a reference process to which the Higgs production channel could be calibrated. For simplicity, we compare our predictions for the two processes at the partonic level, for $\sqrt{\hat{s}} = 500$ GeV. Fig. 8 shows the results for the dominant partonic processes

$$u + d \longrightarrow d + h/Z + u,$$

where (s)fermionic loop corrections are included. The partonic cross section for Z boson production is larger than that for h production, by a factor of ~ 10 (this is also the case in the Standard Model). The loop corrections for the two processes act in the same direction, leading to a slight reduction of the respective cross sections. The loop corrections are at the percent level, where the effects on the light Higgs production cross section are somewhat larger, and (as expected) the light Higgs production cross section is more sensitive to the parameters M_A and $\tan\beta$.

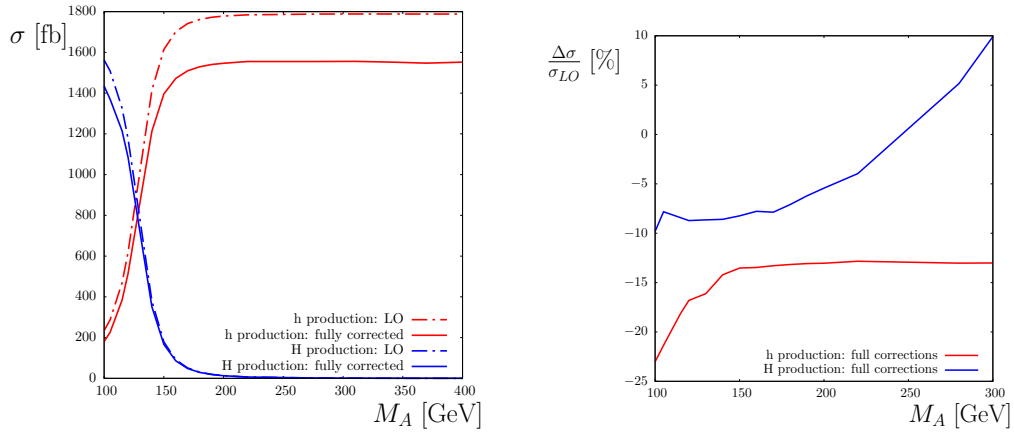

(a) A comparison of production of the light and heavy $\mathcal{CP}$-even Higgs bosons as a function of M_A.

(b) Loop correction percentages as a function of M_A.

Figure 9: Production of the light and heavy $\mathcal{CP}$-even Higgs bosons in the $M_h^{\max}$ scenario, with $\tan\beta = 10$.

While up to now we have concentrated on the production of the light MSSM Higgs boson in WBF, we now compare the cross sections for production of the light, h, and the heavy, H, $\mathcal{CP}$-even Higgs bosons of the MSSM. Fig. 9 shows a comparison of the production cross sections in the $M_h^{\max}$ scenario of the light and the heavy $\mathcal{CP}$-even Higgs, as a function of the mass of the $\mathcal{CP}$-odd Higgs, M_A, with $\tan\beta = 10$, where our 'fullest' corrections have been included (i.e. we neglect only the SUSY-QCD contributions and the box and pentagon type contributions from charginos and neutralinos). At low values of M_A, in the non-decoupling regime where the heavy $\mathcal{CP}$-even Higgs boson has SM-type couplings to gauge bosons, production of the heavy Higgs is the dominant process. This cross section rapidly decreases with in-

creasing M_A, and becomes close to zero in the decoupling regime where the light Higgs h becomes SM-like. Due to this strong suppression of the leading order cross section, the percentage corrections to heavy Higgs production increase in the decoupling regime, although the total cross section is still, of course, relatively small[14]. For the heavy Higgs the loop corrections in the $M_h^{\rm max}$ scenario tend to increase the cross section in the decoupling region (see Ref. [18] for a discussion of scenarios where a much larger enhancement of the heavy Higgs production cross section is possible). For small values of M_A the corrections to the heavy Higgs production cross section reach approximately -10%.

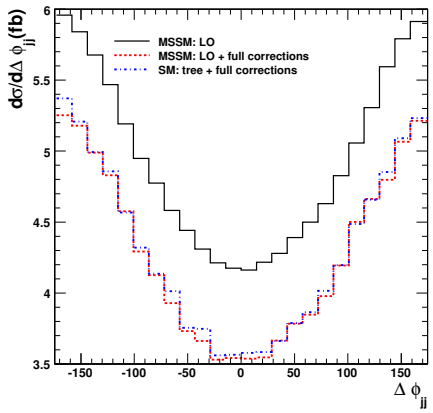

(a) Distribution in the $M_h^{\rm max}$ scenario for h production, with $M_A = 400$ GeV and $M_h = 129.6$ GeV.

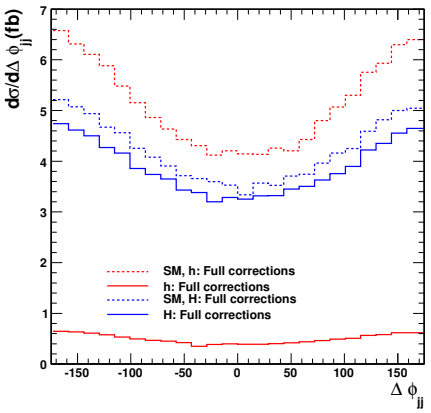

(b) Distribution in the $M_h^{\rm max}$ scenario with $M_A = 100$ GeV for the light $\mathcal{CP}$-even Higgs boson ($M_h = 97.6$ GeV), the heavy $\mathcal{CP}$-even Higgs ($M_H = 133.1$ GeV) and Standard Model Higgs bosons ($M_{H^{SM}} = 97.6$ GeV and $M_{H^{SM}} = 133.1$ GeV) with our most complete corrections included.

Figure 10: Azimuthal angle distributions in the $M_h^{\rm max}$ scenario, with $\tan\beta = 10$.

As an example of a differential distribution, Fig. 10(a) shows the azimuthal angle distribution for h production in the $M_h^{\rm max}$ scenario in the decoupling regime (with $\tan\beta = 10$ and $M_A = 400$ GeV) in comparison with

[14]Note that the right hand plot of Fig. 9 only presents percentage loop corrections for the range $M_A = 100$–300 GeV, where the production cross section of the heavy Higgs is non-negligible.

the corresponding result in the SM with the same value of the Higgs mass, with our most complete corrections included (i.e. in the SM the complete one-loop corrections are included, and in the MSSM only the SUSY-QCD and box and pentagon contributions from charginos and neutralinos are neglected). As expected, h production in the MSSM closely resembles the SM result in this parameter region, so that only small differences occur between the SM and the MSSM results. Moving out of the decoupling regime, the differences between the MSSM and the SM become more significant. This can be seen in Fig. 10(b), which shows a comparison between the SM and the MSSM results for the light and heavy $\mathcal{CP}$-even Higgs bosons in the $M_h^{\max}$ scenario for $M_A = 100$ GeV, again with our fullest corrections included[15]. In this non-decoupling region the cross section of the heavy $\mathcal{CP}$-even Higgs boson is more SM-like than that of the lightest Higgs. While differences in the total rates are clearly visible in this example, the shape of the distribution (which as discussed above contains information about the tensor structure of the coupling between the Higgs and the weak boson pair) in Fig. 10(b) is not significantly altered in the MSSM as compared to the SM case.

4 Conclusions

We have evaluated higher-order corrections to weak boson fusion Higgs production at the LHC in the SM and the MSSM. The weak boson fusion channel is expected to be one of the most important channels for searching for Higgs bosons and for determining the properties of possible Higgs candidates. Our results have been implemented into the public Monte Carlo program `VBFNLO`. Within the SM, a complete one-loop result for weak boson fusion Higgs production has been obtained by evaluating the full virtual electroweak corrections and photon radiation and combining those contributions with the NLO QCD corrections already present in `VBFNLO`. Within the MSSM, the full one-loop SM-type corrections, taking into account the extended Higgs sector of the MSSM, have been combined with the dominant supersymmetric one-loop corrections from the scalar partners of the SM fermions and with propagator-type corrections from the MSSM Higgs sector up to the two-loop level. We have also presented a result where in addition the remaining MSSM contributions to the vertex of the Higgs boson with two gauge bosons, to the gauge

[15]The two SM curves in Fig. 10(b) are for SM Higgs bosons with masses matching the light and heavy $\mathcal{CP}$-even Higgs bosons respectively.

boson self-energies and to the quark vertices are incorporated, and we have verified that the numerical impact of the SUSY loop contributions beyond the dominant sfermion loops is insignificant. Our results have been obtained for the general case of the MSSM with arbitrary complex parameters. The remaining supersymmetric contributions at the one-loop level, namely contributions from neutralinos and charginos to boxes and pentagons as well as the gluino-exchange contributions, are expected to have a small numerical effect, except possibly in the region of a rather light gluino. Results for those contributions will be presented elsewhere. Besides the weak boson fusion Higgs production channel, we have also investigated loop corrections from fermions and their scalar superpartners to Z-boson production in weak boson fusion, which in principle could be of interest as a reference process to which the Higgs production channel could be calibrated.

For those parts of our work where results already exist in the literature we have performed detailed comparisons. For the SM case, we find complete agreement with the results of Ref. [24] within the numerical uncertainties. For the case of the purely supersymmetric corrections to weak boson fusion with real parameters we performed a comparison of the contributions to the Higgs vertex with two gauge bosons both for the default settings of our code and for a "tuned result" where the higher-order corrections in the Higgs sector have been treated in the same way as in Ref. [26]. The numerical results in Ref. [26] are all given for parameters corresponding to the decoupling limit of the MSSM, where the impact of loop corrections affecting the production of the light $\mathcal{CP}$-even Higgs boson is expected to be small. We found that the very small corrections at the level of a fraction of a percent reported in Ref. [26] are due to sizable cancellations between the universal propagator-type corrections and the genuine vertex corrections. For our tuned result we find good agreement with the results obtained in Ref. [26], within the expected uncertainties.

Within the SM, after applying the standard WBF cuts, we find that the electroweak corrections give rise to a downward shift in the cross section of order 5% for a Higgs of mass 100–200 GeV. This is approximately the same size as the QCD NLO corrections in this region of parameter space, leading to a full NLO correction of order -10%. Concerning the production of the light $\mathcal{CP}$-even Higgs boson in the MSSM, the effects caused by loops involving supersymmetric particles are generally small in the decoupling limit, as expected. Comparison of our results for the MSSM and the SM (with the corresponding value of the SM Higgs mass) shows that in this limit the

SM result is indeed recovered from the MSSM prediction to good accuracy. Away from the decoupling region, on the other hand, the genuine vertex corrections in the MSSM show a different behaviour compared to those in the SM, and loops involving supersymmetric particles give rise to corrections in excess of 10%. In fact, approximating the MSSM prediction by the SM result scaled with an effective coupling factor yields only satisfactory results in the decoupling region, while for smaller values of M_A deviations of up to about 15% are possible. Particularly large effects on the Higgs production cross section are possible in the ($\mathcal{CP}$-violating) CPX benchmark scenario. The loop corrections to the Z production process in weak boson fusion are in general smaller than for Higgs production and tend to go into the same direction.

In the non-decoupling region, the heavy $\mathcal{CP}$-even MSSM Higgs boson becomes more SM-like, and the production of the heavy Higgs dominates over the production of the light Higgs for very small M_A. In this region, we find corrections to heavy Higgs production of about -10%. In the numerical examples that we have analysed we find a partial cancellation between electroweak and QCD corrections to the production of the heavy $\mathcal{CP}$-even MSSM Higgs in weak boson fusion in this region. For larger values of M_A, where heavy Higgs production becomes suppressed, the relative corrections change sign and increase with increasing M_A.

The implementation of our results in `VBFNLO` provides a fast and efficient tool for studying cross sections and differential distributions based on state-of-the-art predictions in the SM and the MSSM including the effects of experimental cuts. In this context our approach of parametrising the loop contributions to the vertex of the Higgs boson with two gauge bosons in terms of an effective coupling turned out to be a computationally very efficient way of implementing this part of the calculation. The effective coupling correction was combined with the full $2 \to 3$ matrix element including the remaining loop contributions. The version of `VBFNLO` incorporating our results will be distributed with the next release.

5 Acknowledgments

We would like to thank A. Denner, H. Rzehak and W. Hollik for useful discussions. We are very grateful to M. Rauch for assistance with the SUSY comparisons, and to P. Gonzalez for formfactor comparisons. TF would

also like to thank the Galileo Galilei Institute for Theoretical Physics for the hospitality and the INFN for partial support during part of this work. Work supported in part by the European Community's Marie-Curie Research Training Network under contract MRTN-CT-2006-035505 'Tools and Precision Calculations for Physics Discoveries at Colliders' (HEPTOOLS) and MRTN-CT-2006-035657 'Understanding the Electroweak Symmetry Breaking and the Origin of Mass using the First Data of ATLAS' (ARTEMIS).

References

[1] The ATLAS Collaboration, G. Aad *et al.*, arXiv:0901.0512 [hep-ex].

[2] The CMS Collaboration, G. Bayatian *et al.*, Journal of Physics G: Nuclear and Particle Physics **34**, 995 (2007).

[3] T. Figy, C. Oleari, and D. Zeppenfeld, Phys. Rev. **D68**, 073005 (2003), hep-ph/0306109.

[4] The ILC Collaboration, G. Aarons *et al.*, (2007), arXiv:0709.1893 [hep-ph].

[5] CLIC Physics Working Group, E. Accomando *et al.*, (2004), hep-ph/0412251.

[6] J. R. Espinosa and J. F. Gunion, Phys. Rev. Lett. **82**, 1084 (1999), hep-ph/9807275.

[7] T. Plehn, D. L. Rainwater, and D. Zeppenfeld, Phys. Rev. Lett. **88**, 051801 (2002), hep-ph/0105325.

[8] M. Dührssen, CERN Report No. ATL-PHYS-2003-030, 2003 (unpublished).

[9] M. Dührssen, C. S. Heinemeyer, H. Logan, D. Rainwater, G. Weiglein, and D. Zeppenfeld, Phys. Rev. **D70**, 113009 (2004), hep-ph/0406323.

[10] M. Spira, Fortsch. Phys. **46**, 203 (1998), hep-ph/9705337.

[11] T. Han, G. Valencia, and S. Willenbrock, Phys. Rev. Lett. **69**, 3274 (1992), hep-ph/9206246.

[12] T. Figy and D. Zeppenfeld, Phys. Lett. **B591**, 297 (2004), hep-ph/0403297.

[13] E. L. Berger and J. M. Campbell, Phys. Rev. **D70**, 073011 (2004), hep-ph/0403194.

[14] J. Vollinga, Nucl. Phys. Proc. Suppl. **186**, 102 (2009), arXiv:0809.3693 [hep-ph].

[15] J. R. Andersen, T. Binoth, G. Heinrich, and J. M. Smillie, JHEP **02**, 057 (2008), arXiv:0709.3513 [hep-ph].

[16] A. Bredenstein, K. Hagiwara, and B. Jager, Phys. Rev. **D77**, 073004 (2008), arXiv:0801.4231 [hep-ph].

[17] P. Bolzoni, F. Maltoni, S.-O. Moch, and M. Zaro, arXiv:1003.4451 [hep-ph].

[18] T. Hahn, S. Heinemeyer, and G. Weiglein, Nucl. Phys. **B652**, 229 (2003), hep-ph/0211204v2.

[19] H. Eberl, W. Majerotto, and V. C. Spanos, Phys. Lett. **B538**, 353 (2002), hep-ph/0204280.

[20] G. Belanger *et al.*, Phys. Lett. **B559**, 252 (2003), hep-ph/0212261.

[21] A. Denner, S. Dittmaier, M. Roth, and M. M. Weber, Phys. Lett. **B560**, 196 (2003), hep-ph/0301189.

[22] A. Denner, S. Dittmaier, M. Roth, and M. M. Weber, Nucl. Phys. **B660**, 289 (2003), hep-ph/0302198.

[23] M. Ciccolini, A. Denner, and S. Dittmaier, Phys. Rev. Lett. **99**, 161803 (2007), arXiv:0707.0381 [hep-ph].

[24] M. Ciccolini, A. Denner, and S. Dittmaier, Phys. Rev. **D77**, 013002 (2008), arXiv:0710.4749 [hep-ph].

[25] A. Denner, S. Dittmaier, and A. Mück, HAWK, a Monte Carlo program available at: http://omnibus.uni-freiburg.de/∼sd565/programs/hawk/hawk.html, 2010.

[26] W. Hollik, T. Plehn, M. Rauch, and H. Rzehak, Phys. Rev. Lett. **102**, 091802 (2009), arXiv:0804.2676 [hep-ph].

[27] M. Rauch, W. Hollik, T. Plehn, and H. Rzehak, PoS **RADCOR2009**, 044 (2009), arXiv:1004.2169 [hep-ph].

[28] A. Djouadi and M. Spira, Phys. Rev. **D62**, 014004 (2000), hep-ph/9912476.

[29] K. Arnold *et al.*, Comput. Phys. Commun. **180**, 1661 (2009), arXiv:0811.4559 [hep-ph].

[30] S. Heinemeyer, W. Hollik, and G. Weiglein, Comput. Phys. Commun. **124**, 76 (2000), hep-ph/9812320.

[31] S. Heinemeyer, W. Hollik, and G. Weiglein, Eur. Phys. J. **C9**, 343 (1999), hep-ph/9812472.

[32] G. Degrassi, S. Heinemeyer, W. Hollik, P. Slavich, and G. Weiglein, Eur. Phys. J. **C28**, 133 (2003), hep-ph/0212020.

[33] M. Frank, T. Hahn, S. Heinemeyer, W. Hollik, H. Rzehak, and G. Weiglein, JHEP **02**, 047 (2007), hep-ph/0611326.

[34] S. Heinemeyer, W. Hollik, H. Rzehak, and G. Weiglein, Phys. Lett. **B652**, 300 (2007), arXiv:0705.0746 [hep-ph].

[35] T. Hahn, S. Heinemeyer, W. Hollik, H. Rzehak, and G. Weiglein, Comput. Phys. Commun. **180**, 1426 (2009).

[36] D. Green, hep-ex/0502009.

[37] P. Govoni and C. Mariotti, arXiv:1001.4357 [hep-ph].

[38] T. Hahn, Comput. Phys. Commun. **140**, 418 (2001), hep-ph/0012260.

[39] T. Hahn and C. Schappacher, Comput. Phys. Commun. **143**, 54 (2002), hep-ph/0105349.

[40] T. Hahn and M. Perez-Victoria, Comput. Phys. Commun. **118**, 153 (1999), hep-ph/9807565.

[41] T. Hahn, Comput. Phys. Commun. **178**, 217 (2008), hep-ph/0611273.

[42] T. Hahn and M. Rauch, Nucl. Phys. Proc. Suppl. **157**, 236 (2006), hep-ph/0601248.

[43] T. Hahn and M. Perez-Victoria, Comput. Phys. Commun. **118**, 153 (1999), hep-ph/9807565.

[44] W. Siegel, Phys. Lett. **B84**, 193 (1979).

[45] K. E. Williams and G. Weiglein, Phys. Lett. **B660**, 217 (2008), arXiv:0710.5320 [hep-ph].

[46] S. Dittmaier, Nucl. Phys. **B565**, 69 (2000), hep-ph/9904440.

[47] A. Denner, Fortschr. Phys. **41**, 307 (1993), arXiv:0709.1075 [hep-ph].

[48] K. Hagiwara and D. Zeppenfeld, Nuclear Physics B **313**, 560 (1989).

[49] J. Alwall *et al.*, JHEP **09**, 028 (2007), arXiv:0706.2334 [hep-ph].

[50] S. Heinemeyer, W. Hollik, D. Stockinger, A. M. Weber, and G. Weiglein, JHEP **08**, 052 (2006), hep-ph/0604147.

[51] S. Heinemeyer, W. Hollik, A. M. Weber, and G. Weiglein, JHEP **04**, 039 (2008), arXiv:0710.2972 [hep-ph].

[52] A. D. Martin, R. G. Roberts, W. J. Stirling, and R. S. Thorne, Eur. Phys. J. **C39**, 155 (2005), hep-ph/0411040.

[53] Tevatron Electroweak Working Group and CDF Collaboration and D0 Collaboration, arXiv:0803.1683 [hep-ex].

[54] Particle Data Group, C. Amsler *et al.*, Phys. Lett. **B667**, 1 (2008).

[55] J. R. Andersen and J. M. Smillie, Phys. Rev. **D75**, 037301 (2007), hep-ph/0611281.

[56] K. Arnold, T. Figy, B. Jager, and D. Zeppenfeld, JHEP **08**, 088 (2010), arXiv:1006.4237 [hep-ph].

[57] B. Allanach *et al.*, Eur. Phys. J. **C25**, 113 (2002), hep-ph/0202233.

[58] A. D. Martin, R. G. Roberts, W. J. Stirling, and R. S. Thorne, Eur. Phys. J. **C28**, 455 (2003), hep-ph/0211080.

[59] V. Hankele, G. Klamke, D. Zeppenfeld, and T. Figy, Phys. Rev. **D74**, 095001 (2006), hep-ph/0609075.

[60] C. Ruwiedel, N. Wermes, and M. Schumacher, Eur. Phys. J. **C51**, 385 (2007).

[61] M. S. Carena, S. Heinemeyer, C. E. M. Wagner, and G. Weiglein, Eur. Phys. J. **C26**, 601 (2003), hep-ph/0202167.

[62] LEP Working Group for Higgs boson searches Collaboration, S. Schael *et al.*, Eur. Phys. J. **C47**, 547 (2006), hep-ex/0602042.

[63] S. Heinemeyer, W. Hollik, and G. Weiglein, Eur. Phys. J. **C16**, 139 (2000), hep-ph/0003022.